



Contents lists available at ScienceDirect

## Bioorganic &amp; Medicinal Chemistry Letters

journal homepage: [www.elsevier.com/locate/bmcl](http://www.elsevier.com/locate/bmcl)

# Identification of a novel selective small-molecule inhibitor of protein arginine methyltransferase 5 (PRMT5) by virtual screening, resynthesis and biological evaluations

Kongkai Zhu<sup>a,c</sup>, Chengshi Jiang<sup>a,c</sup>, Hongrui Tao<sup>a</sup>, Jingqiu Liu<sup>b</sup>, Hua Zhang<sup>a,\*</sup>, Cheng Luo<sup>b,\*</sup>

<sup>a</sup> School of Biological Science and Technology, University of Jinan, Jinan 250022, PR China

<sup>b</sup> Drug Discovery and Design Center, State Key Laboratory of Drug Research, Shanghai Institute of Materia Medica, Chinese Academy of Sciences, Shanghai 201203, PR China

## ARTICLE INFO

## Article history:

Received 23 February 2018

Accepted 29 March 2018

Available online xxxx

## Keywords:

PRMT5 inhibitor

Resynthesis

Virtual screening

Molecular docking

Molecular dynamics simulation

## ABSTRACT

As one of the most promising anticancer target in protein arginine methyltransferase (PRMT) family, PRMT5 has been drawing more and more attentions, and many efforts have been devoted to develop its inhibitors. In this study, three PRMT5 inhibitors (**9**, **16**, and **23**) with novel scaffolds were identified by performing pharmacophore- and docking-based virtual screening combined with *in vitro* radiometric-based scintillation proximity assay (SPA). Substructure search based on the scaffold of the most active **9** afforded 26 additional analogues, and SPA results indicated that two analogues (**9-1** and **9-2**) showed increased PRMT5 inhibitory activity compared with the parental compound. Resynthesis of **9**, **9-1**, and **9-2** confirmed their PRMT5 enzymatic inhibition activity. In addition, compound **9-1** displayed selectivity against PRMT5 over other key homological members (PRMT1 and CARM1 (PRMT4)). While the structure-activity relationship (SAR) of this series of compounds was discussed to provide clues for further structure optimization, the probable binding modes of active compounds were also probed by molecular docking and molecular dynamics simulations. Finally, the antiproliferative effect of **9-1** on MV4-11 leukemia cell line was confirmed and its impact on regulating the target gene of PRMT5 was also validated. The hit compounds identified in this work have provided more novel scaffolds for future hit-to-lead optimization of small-molecule PRMT5 inhibitors.

© 2018 Elsevier Ltd. All rights reserved.

Protein arginine methyltransferases (PRMTs) play important roles in diverse and essential biological processes including cell growth, cell proliferation, cell cycle regulation, cell death,<sup>1,2</sup> gene transcription,<sup>3</sup> RNA splicing,<sup>4,5</sup> ribosome biogenesis,<sup>6</sup> kinase signalling,<sup>7</sup> etc. Nine members (PRMT1–9) of mammalian PRMTs have been identified and demonstrated to fulfil their functions by methylating arginine residues of their cytoplasm and nuclear substrate proteins.<sup>8</sup> Modification of histone is the most important function of PRMTs, which represents a significant component accounting for the complexity of the overall epigenetic system.<sup>9</sup> By catalysing the methylation of nucleosomal histone tails, PRMTs participate in the regulation of the adaptive switching between transcriptionally active and silent chromatin states.<sup>10,11</sup> Dysregulation or aberrant expression of PRMTs are associated with a variety of human diseases especially cancer. For example, PRMT1,<sup>12–13</sup> 3,<sup>12–4</sup>,<sup>12</sup> and -7,<sup>14</sup> are found overexpressed or aberrant in breast

cancer; both PRMT1 and PRMT5 are overexpressed in lung cancer and leukaemia<sup>12</sup>; PRMT6 accumulates in bladder and lung cancer<sup>12</sup>; PRMT9 is involved in lymphoma, melanoma, testicular, and pancreatic cancers.<sup>15</sup> Owing to the pivotal roles of PRMTs in the occurrence and progression of tumor, they have recently received more and more attention and become an important and promising class of anticancer targets.<sup>9</sup> Up to date, quite a few micromolar and submicromolar small-molecule inhibitors have been obtained for nearly all PRMT members, especially for those key ones such as PRMT1, CARM1 (PRMT4), and PRMT5.<sup>9</sup> Among the reported PRMT1, PRMT3, CARM1, PRMT5, and PRMT6-specific inhibitors, a small molecule (**GSK-3326595**) against PRMT5 has been put into clinical trial<sup>16</sup> indicative of the promising potential of PRMT5 as a good drug development target.

PRMT5 belongs to the symmetric dimethylation enzyme group and can perform the methylation of an arginine residue up to two methyls. This process is assisted by its cofactor methyltransferase protein 50 (MEP50) which has also been known as p44. Histone H4 arginine 3 (H4R3) and histone H3 arginine 8 (H3R8) are two general methylating sites of PRMT5 and can be

\* Corresponding authors.

E-mail addresses: [bio\\_zhangh@ujn.edu.cn](mailto:bio_zhangh@ujn.edu.cn) (H. Zhang), [clu@simmm.ac.cn](mailto:clu@simmm.ac.cn) (C. Luo).<sup>c</sup> These authors contributed equally.

<https://doi.org/10.1016/j.bmcl.2018.03.087>

0960-894X/© 2018 Elsevier Ltd. All rights reserved.

symmetrically dimethylated resulting in repression of gene expression.<sup>17,18</sup> It is shown that PRMT5 promotes cell survival and growth by directly methylating epidermal growth factor receptor (EGFR), E2F1, and p53.<sup>19–22</sup> Studies have indicated that PRMT5 could promote tumorigenesis in multiple tissues by regulating various partners such as p53,<sup>23</sup> cyclin D1,<sup>24</sup> and Janus-activated kinase-2.<sup>25</sup> In addition, in mouse embryonic fibroblast (MEF) cells, PRMT5 can be recruited by Menin to the promoter of growth arrest specific 1 (*Gas1*) gene and suppresses *Gas1* expression.<sup>26</sup> In agreement with its promising anticancer target role, PRMT5 has been found overexpressed in lymphoma, leukemia, and glioblastoma, as well as colorectal, ovarian, lung, and prostate cancers.<sup>27</sup>

In addition to SAM analogues (Chart 1) that are Pan-MTase (methyltransferase) inhibitors, only four classes of PRMT5 inhibitors (Chart 1) have been reported so far.<sup>27–30</sup> Considering the significance of PRMT5 as an anticancer target, the discovery and development of more PRMT5-specific inhibitors remains a pressing task for medicinal chemists.

In this study, six PRMT5 inhibitors of three novel scaffolds were identified with IC<sub>50</sub> values ranging from 14 to 56 μM by employing structure-based virtual screening and radiometric-based scintillation proximity assay (SPA). Resynthesis of top three active compounds **9**, **9-1**, and **9-2** confirmed their PRMT5 enzymatic inhibition activity. Moreover, the most potent compound **9-1** displayed well selectivity with no inhibition against other key PRMT members (PRMT1 and CRAM1). Through molecular docking and molecular dynamics simulations, the binding modes of this series

of active compounds were proposed and their preliminary structure activity relationship (SAR) was also discussed. Cell level assay showed that **9-1** displayed moderate antiproliferative activity against MV4-11 cells with an EC<sub>50</sub> value of 22.5 μM and upregulated the expression of the target gene (*Gas1*) of PRMT5. The present search for new PRMT5 inhibitors has provided new chemical templates for future hit-to-lead optimization and will contribute to further development of new therapeutic candidates for cancer treatment.

## 52 Small-molecule PRMT5 candidate inhibitors were obtained by pharmacophore- and docking-based virtual screening

Pharmacophore- and docking-based virtual screening was used to screen small-molecule PRMT5 candidate inhibitors. Crystal structure of human PRMT5 had been determined by X-ray diffraction and deposited in RCSB protein data bank (PDB), which laid the foundation for structure-based virtual screening targeting PRMT5. At present, there are ten human PRMT5 crystal structures available in PDB with codes of 5C9Z, 5EMJ,<sup>31</sup> 5EMK,<sup>31</sup> 5EML,<sup>31</sup> 5EMM,<sup>31</sup> 5FA5,<sup>32</sup> 4X60,<sup>28</sup> 4X61,<sup>28</sup> 4X63,<sup>28</sup> and 4GQB,<sup>33</sup> respectively, and all structures are in the form of PRMT5:MEP50 complex with different ligands in SAM and substrate binding sites. Among these crystal structures, only 5EML and 4X61 contain the cofactor SAM, while 4GQB is the sole one incorporating a histone H4 peptide at the substrate binding site. 5EML with higher resolution (2.39 Å) than 4X61 (2.85 Å) and 4GQB (2.06 Å) was eventually chosen in the virtual

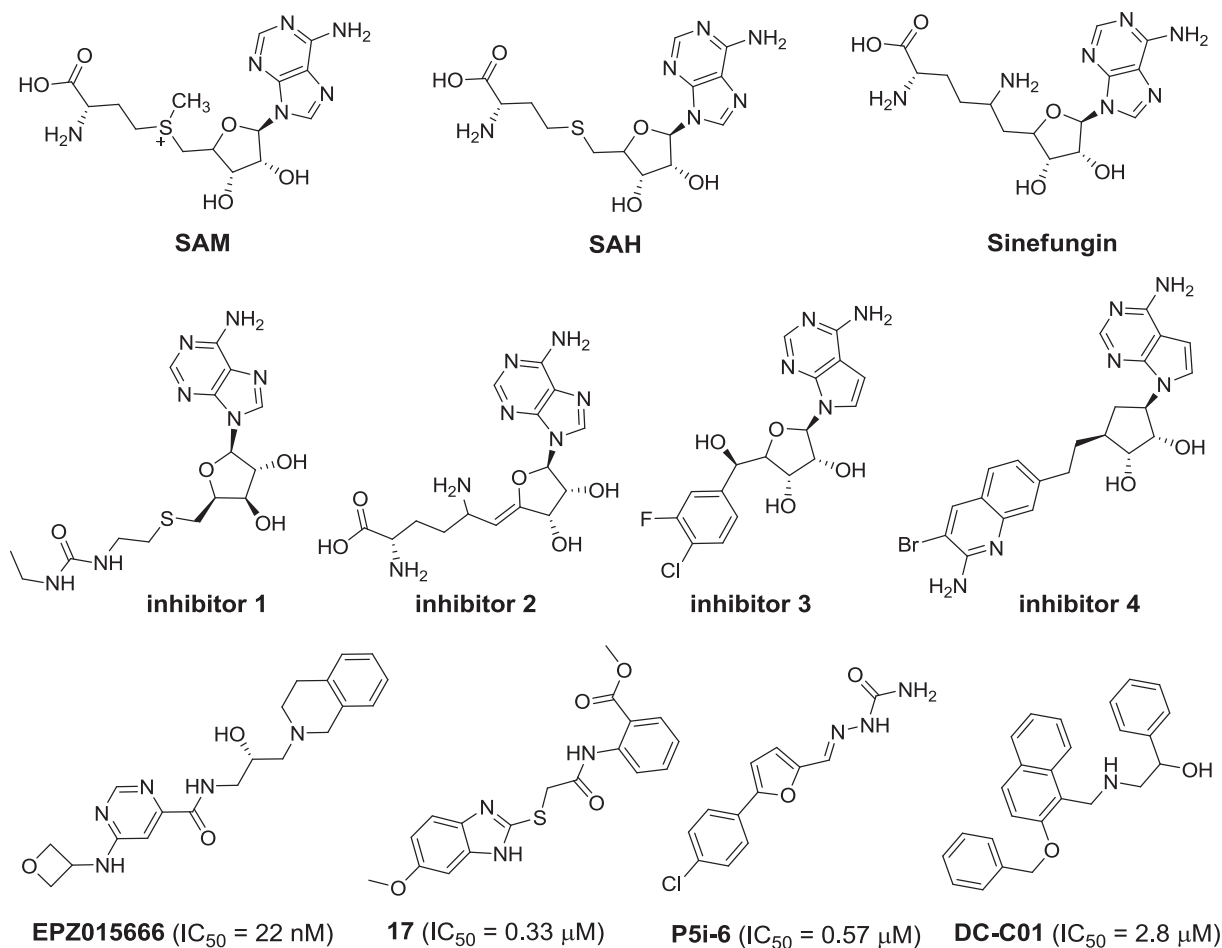


Chart 1. Reported PRMT5 inhibitors.

screening for new inhibitors targeting SAM binding sites. In the constructed structure, the coordinates of PRMT5:MPE50 and SAM were derived from 5EML while the H4 peptide was derived from 4GQB. The screening workflow (Fig. 1A) was as follows. First, based

on the constructed structure of PRMT5, a pharmacophore model (Fig. 1B) was mimicked with nine features consisting of two hydrogen bond donors (HB\_Donor1 and HB\_Donor5), four hydrogen bond acceptors (HB\_Acceptor2, HB\_Acceptor3, HB\_Acceptor4, and

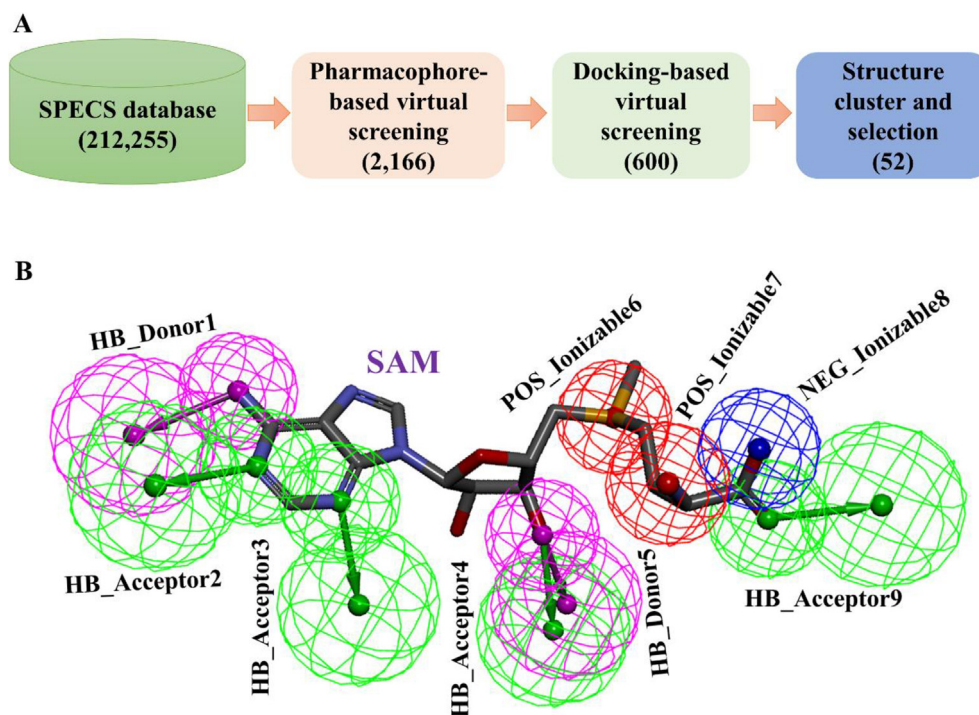


Fig. 1. (A) Workflow of the virtual screening strategy adopted in the present study; (B) The diagram of pharmacophore model aligned with SAM.

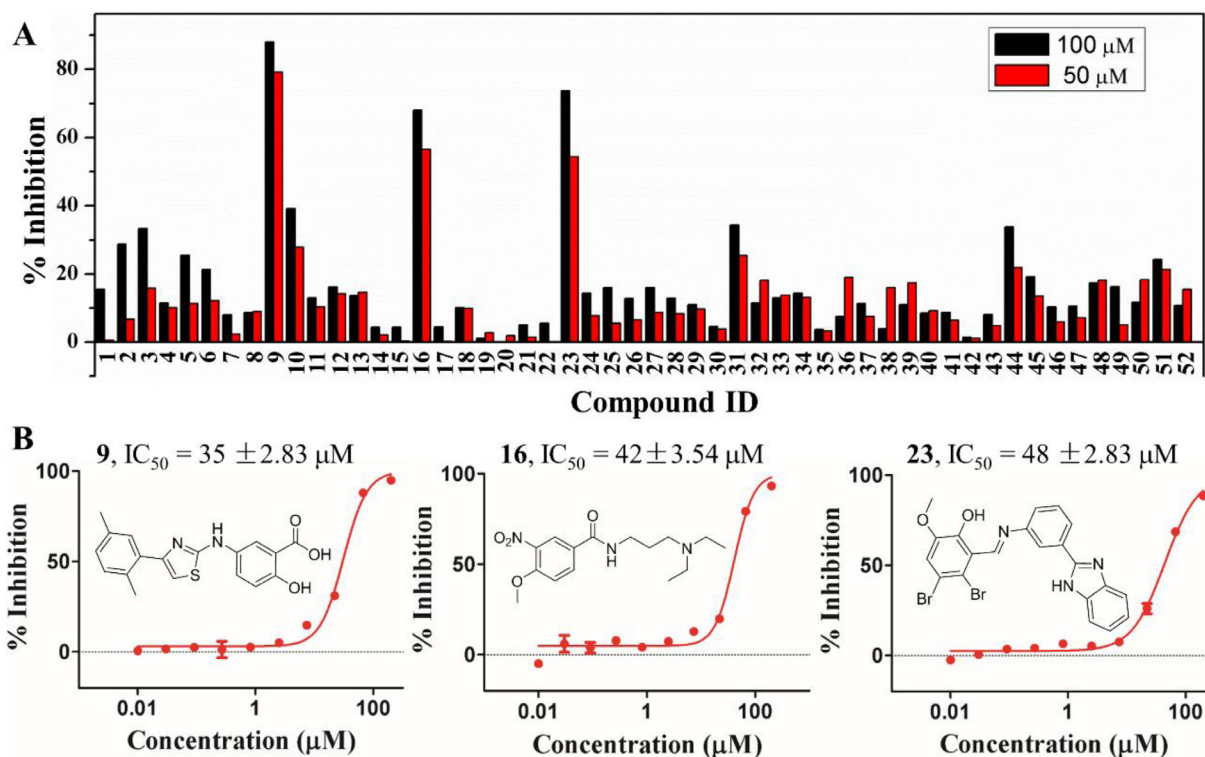
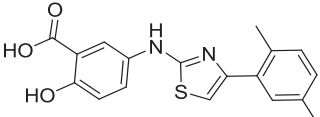
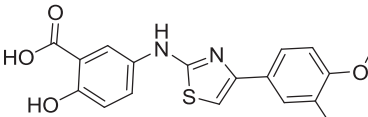
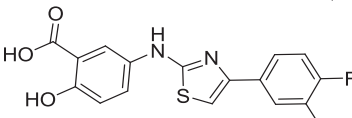
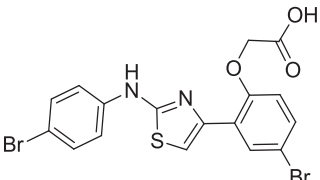


Fig. 2. (A) Inhibitory activities of the 52 PRMT5 candidate inhibitors at 100 and 50  $\mu\text{M}$ , respectively. (B) The structures and  $\text{IC}_{50}$  values of the hit compounds. Data shown are mean  $\pm$  SD of three replicates.

HB\_Acceptor9), and two positive (POS\_Ionizable6 and POS\_Ionizable7) and one negative ionizables (NEG\_Ionizable8). This model was then used to screen SPECS database (<http://www.specs.net>) containing 212,255 compounds, and a total of 2166 candidates that matched at least four above-mentioned pharmacophore features were obtained. Next, the 2166 candidates were further docked into SAM binding sites of PRMT5 by molecular docking to remove com-

pounds with low binding scores. The top 600 small molecules ranked by the XP Gscore were acquired for the subsequent cluster analysis and manual selection. Finally, according to cluster results and the selection criteria that we previously reported,<sup>27</sup> 52 small-molecule PRMT5 inhibitor candidates were selected and purchased for further biological evaluation against the methylation activity of PRMT5.

**Table 1**  
Inhibitory activity of **9** and its three analogues (**9-1** to **9-3**) against PRMT5.<sup>a</sup>

Compounds	Structure	Inhibition rate (%)	IC <sub>50</sub> (μM)
<b>9</b>		80.0	35 ± 2.83
<b>9-1</b>		95.0	14 ± 1.41
<b>9-2</b>		71.0	22 ± 0.19
<b>9-3</b>		61.0	44 ± 2.26

<sup>a</sup> Initial inhibition rate was tested at 50 μM for all compounds, and only those with <50% inhibition rate were selected for IC<sub>50</sub> measurements. Data shown are mean ± SD of three replicates.

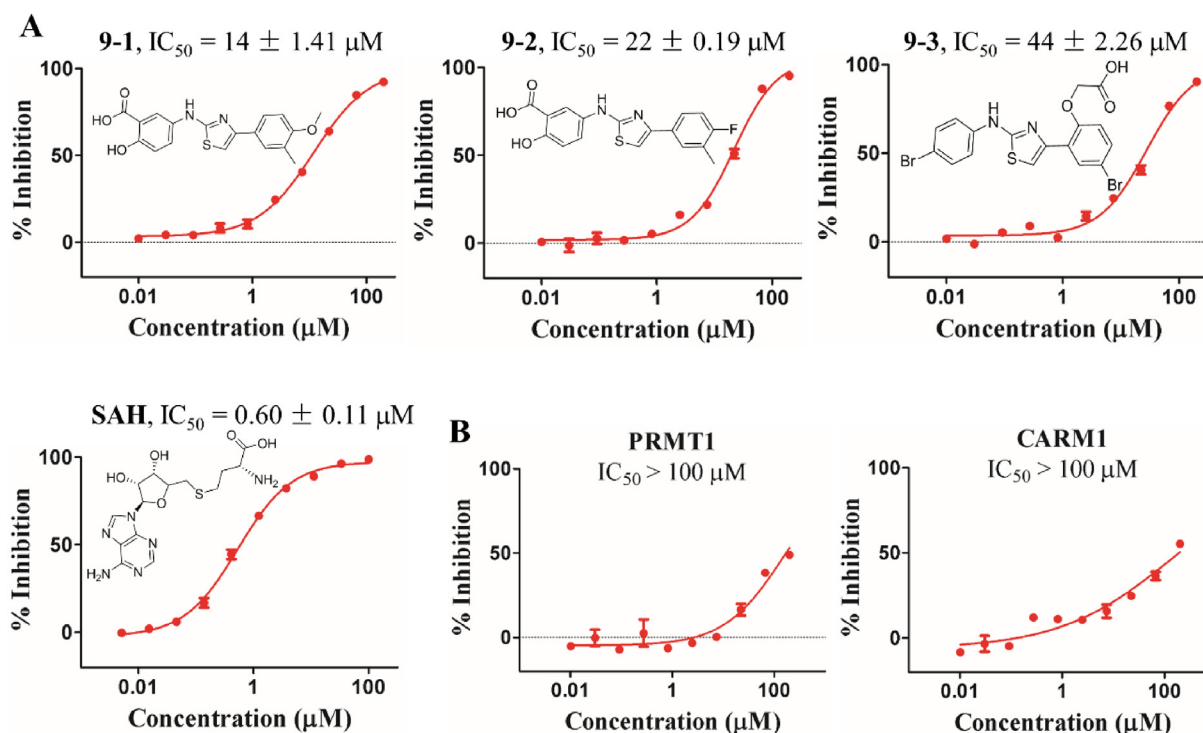


**Fig. 3.** (A) The structures and IC<sub>50</sub> values of the three active analogues of compound **9** and the positive control SAH. (B) IC<sub>50</sub> determination of **9-1** against PRMT1 and CARM1 using SPA method. Data shown are mean ± SD of three replicates.

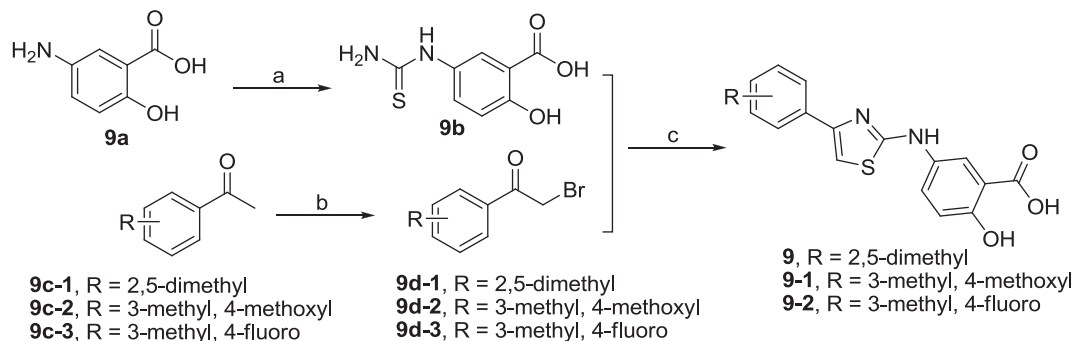
### Radiometric-based SPA results revealed three candidates with PRMT5 inhibitory activity at enzymatic level

Radiometric-based assay has become a highly accepted protocol for quantitating *in vitro* activity of PRMTs owing to its high sensitivity. In this work, radiometric-based SPA was used to detect the inhibitory activity of the 52 candidates against PRMT5 at enzymatic level. The inhibition rate of each candidate was tested at the concentrations of 100 and 50  $\mu\text{M}$ , respectively. SPA results showed that three compounds displayed inhibition rate above 50% at 100  $\mu\text{M}$  (Fig. 2A), and the  $\text{IC}_{50}$  values of them were then determined and shown in Fig. 2B. As we can see, the three active compounds represented three different scaffolds with  $\text{IC}_{50}$  values

ranging from 35 to 56  $\mu\text{M}$ , of which **9** exhibited the most potent inhibitory activity.

### Two of 26 analogues displayed better PRMT5 inhibitory activity than **9** and their SAR was discussed

As **9** showed the best activity among the aforementioned three candidates, similarity search was performed to retrieve its analogues for further evaluation. Then 26 analogues in SPECS database were collected and their PRMT5 inhibitory activities were tested. The assay results were summarized in Tables 1 and S1. As shown (Fig. 3A), two analogues, i.e. **9-1** and **9-2**, showed better activity than **9** with  $\text{IC}_{50}$  values of 14 and 22  $\mu\text{M}$ , respectively, while the



**Scheme 1.** Synthesis of **9**, **9-1**, and **9-2**. Reagents and conditions: (a) i) Benzoyl isothiocyanate, acetone, rt; ii) 1 N NaOH(aq), THF, reflux; (b)  $\text{PhMe}_3\text{NBr}_3$ , THF; (c) EtOH, reflux.

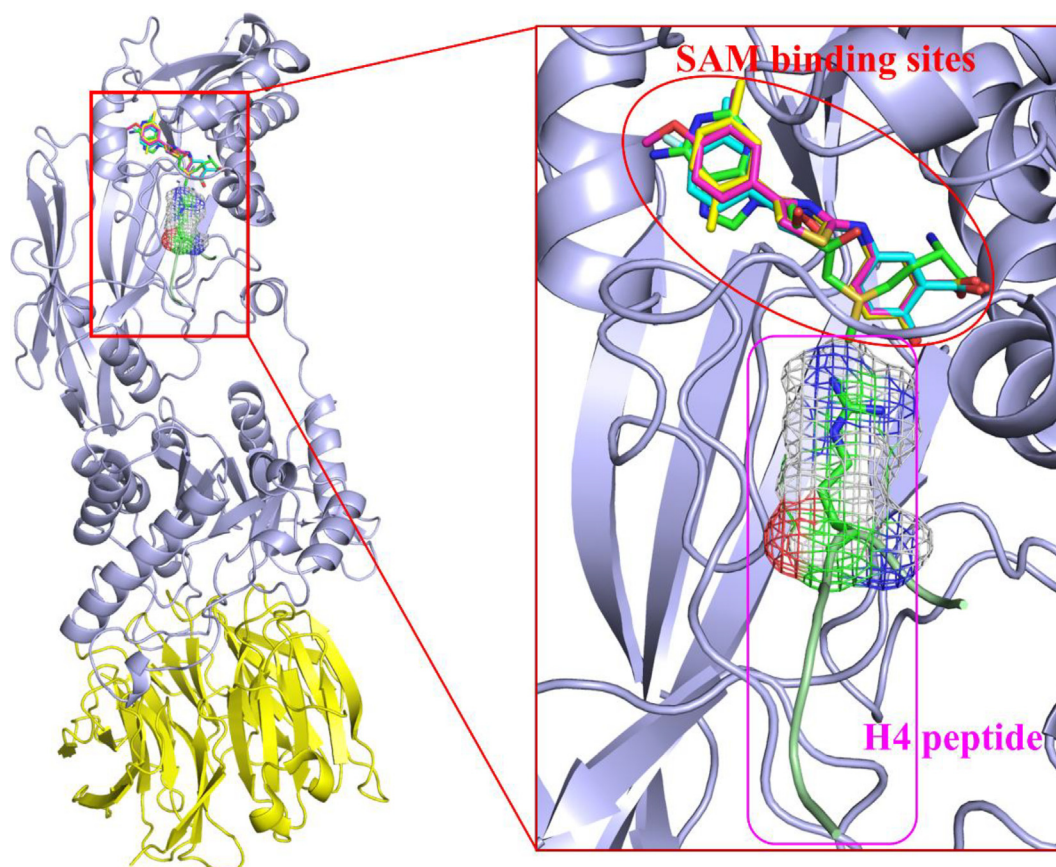


**Fig. 4.** Binding modes of compounds **9**, **9-1**, and **9-2** with PRMT5. PRMT5 and MEP50 are shown in cartoon diagram in purplish and yellow, respectively. Compounds **9**, **9-1**, and **9-2** occupy the SAM binding site represented as yellow, magenta, and cyan sticks, respectively, while SAM is shown as green sticks. Arginine residue 3 in H4 peptide is also shown as green sticks.

third one (**9-3**) exhibited decreased activity with an  $IC_{50}$  value of 44  $\mu$ M. S-adenosyl homocysteine (SAH) was used as the positive control when testing the  $IC_{50}$  values of the targeted compounds. Based on the structures and activities of this series of compounds, their SAR was discussed as follows: 1) The carboxylic acid group appeared to be an essential factor for their activity and was speculated to interact with the key residues K333 and Y334 of the SAM binding sites of PRMT5, which was further validated by later analysis of their proposed binding modes. The only exception was the thiazolium salt **9-4**. 2) Replacement of the hydroxybenzoic acid moiety by alkoxy- and halogen-substituted benzene rings (**9-5** to **9-13**) or benzo[*b*]thiophene-dioxide ring (**9-14**) dramatically reduced the inhibition rates to the range of 20–33% at 50  $\mu$ M, presumably due to the loss of H-bond or salt bridge interaction with the key residues Y334, K333, and E435. 3) Substitution of the 4-benzene fragment of thiazole moiety by more bulky aromatic rings, such as benzofuran (**9-15**), naphthalene (**9-16**), coumarin (**9-17** to **9-19**), and benzyloxyphenyl (**9-20** and **9-21**) led to the loss of activity (inhibition rates <10%). In addition, to expand the structural diversity of tested compounds, five more analogues with benzamido (**9-22** to **9-24**) or benzoylthioureido (**9-25** and **9-26**) were also screened, but none of them showed inhibitory activity against PRMT5.

### Resynthesis of **9**, **9-1**, and **9-2** confirmed their PRMT5 inhibitory activity

The top three active compounds **9**, **9-1**, and **9-2** were synthesized to further confirm their PRMT5 enzymatic inhibition activity.

The synthetic strategy for target compounds **9**, **9-1**, and **9-2** is depicted in Scheme 1. Briefly, thiourea **9b** was prepared by starting from aniline **9a** and benzoyl isothiocyanate in two steps according to a previously reported protocol.<sup>34</sup>  $\alpha$ -Bromoacetophenones **9d** were generally obtained from corresponding aceto compounds **9c** and phenyltrimethylammonium tribromide. Finally, aminothiazole formations<sup>34</sup> of **9b** and **9c** generated the target compounds **9**, **9-1**, and **9-2**.

### Compound **9-1** showed selective inhibitory activity against PRMT5

The most active **9-1** was chosen for further test on its inhibition against two other key homological members of PRMT5, PRMT1 and CARM1. As shown in Fig. 3B, the assay results revealed that **9-1** was inactive toward the latter two enzymes with  $IC_{50}$  values larger than 100  $\mu$ M, which suggested that this class of compounds were selective PRMT5 inhibitors.

**Table 2**

The binding free energy of **9**, **9-1** and **9-2** to PRMT5 calculated by the MM/PBSA method.<sup>a</sup>

	$\Delta G_{\text{gas}}$	$\Delta G_{\text{solv}}$	$\Delta G$
<b>9</b>	-11.50	-8.21	-19.71
<b>9-1</b>	-14.74	-22.55	-37.29
<b>9-2</b>	-21.08	-8.24	-29.32

<sup>a</sup> All calculated values were given in kcal/mol.  $\Delta G = \Delta G_{\text{gas}} + \Delta G_{\text{solv}}$ .  $\Delta G_{\text{gas}}$  represents the binding free energy in vacuum while  $\Delta G_{\text{solv}}$  represents the solvation free energy change.

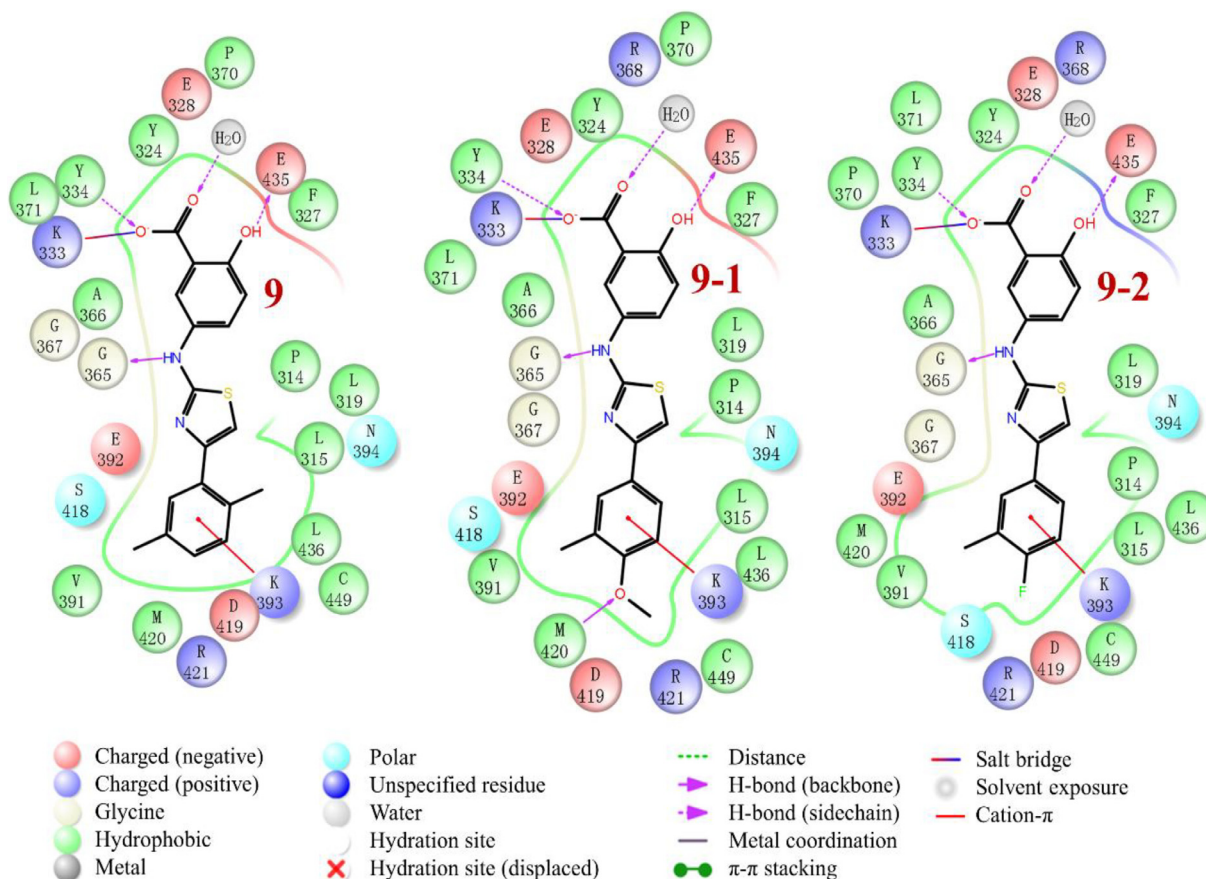


**Fig. 5.** The detailed interactions of compounds **9**, **9-1**, and **9-2** with PRMT5.

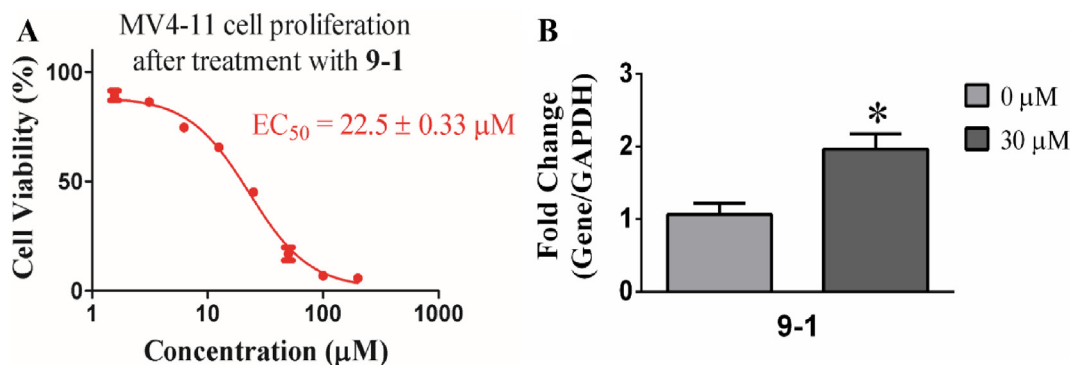


**Fig. 6.** (A) Effect of compound **9-1** on the proliferation of MV4-11 cells; (B) RT-qPCR analysis of the gene expression of *Gas1* when treated with **9-1** at 30  $\mu\text{M}$ . Results shown are mean  $\pm$  SD of three replicates. \* $P < 0.05$ .

### Binding modes of the active compounds to PRMT5 were obtained by molecular docking and verified by molecular dynamics simulation

As shown in Figs. 4 and S1, molecular docking was used to acquire the binding modes of **9**, **9-1**, **9-2**, and **9-3**, with reasonable binding poses similar to that of SAM. It was interesting to note that first three compounds showed exactly the same binding modes, whereas the *N*-phenyl ring in **9-3** displayed opposite spatial orientation leading to reduced interactions (Fig. S2) with PRMT5, which could be responsible for its lower activity. The detailed interactions of **9**, **9-1**, and **9-2** with PRMT5 were shown in Fig. 5. As can be observed, hydrophobic, hydrogen bond, salt bridge, and cation- $\pi$  interactions were the main forces in stabilizing the binding conformation. Not surprisingly, **9-1** showed an extra hydrogen bond with Met420 residue of PRMT5, which might be a significant factor accounted for its best activity among these analogues. To further analyse the reason of **9** and **9-2** showing different activities, molecular dynamics (MD) simulation was used to obtain more information on their SAR. 100 ns MD simulation was thus performed on the complexes of **9**, **9-1**, and **9-2** with PRMT5:MEP50. By calculating the binding free energy using MM/PBSA method based on their MD trajectories, **9**, **9-1**, and **9-2** were demonstrated to have different binding affinity (Table 2) to PRMT5 with values of  $-19.71$ ,  $-37.29$ , and  $-29.32$  kcal/mol, respectively. The binding free energy order of these three compounds was in well agreement with their experimental activities.

### Compound **9-1** showed antiproliferative activity on MV4-11 cells and exhibited impact on the target gene of PRMT5

PRMT5 was validated as anticancer target and found overexpressed in leukemia, so MV4-11 leukemia cell was used to test the antiproliferation effect of the most active **9-1**. As shown in Fig. 6A, **9-1** displayed concentration-dependent antiproliferative effect on MV4-11 cells with a 4-day  $\text{EC}_{50}$  value of 22.5  $\mu\text{M}$ . Moreover, *Gas1* was reported to block the proliferation of a variety of cancer cells including lung carcinoma, bladder carcinoma, and glioma,<sup>35</sup> and PRMT5 knockdown in MEF cells would lead to increased levels of *Gas1*.<sup>36</sup> Therefore, we analysed the differential expression of *Gas1* gene by real-time quantitative polymerase chain reaction (RT-qPCR). As shown in Fig. 6B, *Gas1* was significantly upregulated when treated with **9-1** at 30  $\mu\text{M}$  indicating that **9-1** could target PRMT5 in MEF cells.

In conclusion, three novel PRMT5 inhibitors were identified by pharmacophore- and docking-based virtual screening with  $\text{IC}_{50}$  values ranging from 35 to 56  $\mu\text{M}$ . Compared with the previously reported PRMT5 inhibitors, all three hits contained new scaffolds

and could be used for further optimization to improve their activities. 26 analogues of compound **9** in SPECS database were retrieved and purchased, and two of them displayed more potent inhibitory activity against PRMT5 indicated by SPA results. Resynthesis of **9**, **9-1**, and **9-2** confirmed their PRMT5 enzymatic inhibition activity. From the proposed binding modes, the top three active hits (**9**, **9-1**, and **9-2**) had hydrophobic, hydrogen bond, salt bridge and cation- $\pi$  interactions with PRMT5. MD simulation results indicated that the order of the binding free energy was in well agreement with the activity of the three compounds. Finally, the antiproliferative effect of the most active **9-1** was confirmed in MV4-11 cells, and the qPCR results validated the target on PRMT5 of **9-1**. Besides, **9-1** displayed well selectivity against PRMT5 among the key PRMT members (PRMT1, and CARM1). Therefore, the hits discovered in this study will provide novel scaffolds for further hit-to-lead optimization and lay the foundation for further development of therapeutic candidates for cancer treatments.

### Acknowledgements

This work was supported by Natural Science Foundation of Shandong Province [Nos. ZR2017BH038, JQ201721], the Natural Science Foundation of China [21672082], Shandong Key Development Project [No. 2016GSF201209], the Young Taishan Scholars Program [No. tsqn20161037], and Shandong Talents Team Cultivation Plan of University Preponderant Discipline [No. 10027].

### A. Supplementary data

Supplementary data associated with this article can be found, in the online version, at <https://doi.org/10.1016/j.bmcl.2018.03.087>.

### References

- Karkhanis V, Hu YJ, Baiocchi RA, Imbalzano AN, Sif S. Versatility of PRMT5-induced methylation in growth control and development. *Trends Biochem Sci.* 2011;36:633–641.
- Bedford MT, Clarke SG. Protein arginine methylation in mammals: who, what, and why. *Mol Cell.* 2009;33:1–13.
- Wysocka J, Allis CD, Coonrod S. Histone arginine methylation and its dynamic regulation. *Front Biosci.* 2006;11:344–355.
- Deng X, Gu L, Liu C, et al. Arginine methylation mediated by the Arabidopsis homolog of PRMT5 is essential for proper pre-mRNA splicing. *Proc Natl Acad Sci U S A.* 2010;107:19114–19119.
- Sanchez SE, Petrillo E, Beckwith EJ, et al. A methyl transferase links the circadian clock to the regulation of alternative splicing. *Nature.* 2010;468:112–116.
- Ren J, Wang Y, Liang Y, Zhang Y, Bao S, Xu Z. Methylation of ribosomal protein S10 by protein-arginine methyltransferase 5 regulates ribosome biogenesis. *J Biol Chem.* 2010;285:12695–12705.

7. Rust HL, Thompson PR. Kinase consensus sequences: a breeding ground for crosstalk. *ACS Chem Biol.* 2011;6:881–892.
8. Kaniskan HU, Konze KD, Jin J. Selective inhibitors of protein methyltransferases. *J Med Chem.* 2015;58:1596–1629.
9. Hu H, Qian K, Ho MC, Zheng YG. Small molecule inhibitors of protein arginine methyltransferases. *Expert Opin Invest Drugs.* 2016;25:335–358.
10. Strahl BD, Allis CD. The language of covalent histone modifications. *Nature.* 2000;403:41–45.
11. Jenuwein T, Allis CD. Translating the histone code. *Science.* 2001;293:1074–1080.
12. Yang Y, Bedford MT. Protein arginine methyltransferases and cancer. *Nat Rev Cancer.* 2013;13:37–50.
13. Zhong J, Cao RX, Hong T, et al. Identification and expression analysis of a novel transcript of the human PRMT2 gene resulted from alternative polyadenylation in breast cancer. *Gene.* 2011;487:1–9.
14. Yao R, Jiang H, Ma Y, et al. PRMT7 induces epithelial-to-mesenchymal transition and promotes metastasis in breast cancer. *Cancer Res.* 2014;74:5656–5667.
15. Uhlen M, Fagerberg L, Hallstrom BM, et al. Proteomics. Tissue-based map of the human proteome. *Science.* 2015;347:1260419.
16. Zhu K, Jiang CS, Hu J, et al. Interaction assessments of the first S-adenosylmethionine competitive inhibitor and the essential interacting partner methyltransferase 5 with protein arginine methyltransferase 5 by combined computational methods. *Biochem Biophys Res Commun.* 2018;495:721–727.
17. Friesen WJ, Wyce A, Paushkin S, et al. A novel WD repeat protein component of the methyltransferase binds Sm proteins. *J Biol Chem.* 2002;277:8243–8247.
18. Pal S, Vishwanath SN, Erdjument-Bromage H, Tempst P, Sif S. Human SWI/SNF-associated PRMT5 methylates histone H3 arginine 8 and negatively regulates expression of ST7 and NM23 tumor suppressor genes. *Mol Cell Biol.* 2004;24:9630–9645.
19. Jansson M, Durant ST, Cho EC, et al. Arginine methylation regulates the p53 response. *Nat Cell Biol.* 2008;10:1431–1439.
20. Hsu JM, Chen CT, Chou CK, et al. Crosstalk between Arg 1175 methylation and Tyr 1173 phosphorylation negatively modulates EGFR-mediated ERK activation. *Nat Cell Biol.* 2011;13:174–181.
21. Cho EC, Zheng SS, Munro S, et al. Arginine methylation controls growth regulation by E2F-1. *EMBO J.* 2012;31:1785–1797.
22. Zheng SS, Moehlenbrink J, Lu YC, et al. Arginine methylation-dependent reader-writer interplay governs growth control by E2F-1. *Mol Cell.* 2013;52:37–51.
23. Durant ST, Cho EC, La Thangue NB. P53 methylation—the argument is clear. *Cell Cycle.* 2009;8:801–802.
24. Aggarwal P, Vaites LP, Kim JK, et al. Nuclear cyclin D1/CDK4 kinase regulates CUL4 expression and triggers neoplastic growth via activation of the PRMT5 methyltransferase. *Cancer Cell.* 2010;18:329–340.
25. Liu F, Zhao X, Perna F, et al. JAK2V617F-mediated phosphorylation of PRMT5 downregulates its methyltransferase activity and promotes myeloproliferation. *Cancer Cell.* 2011;19:283–294.
26. Gurung B, Feng Z, Iwamoto DV, et al. Menin epigenetically represses Hedgehog signaling in MEN1 tumor syndrome. *Cancer Res.* 2013;73:2650–2658.
27. Mao R, Shao J, Zhu K, et al. Potent, selective, and cell active protein arginine methyltransferase 5 (PRMT5) inhibitor developed by structure-based virtual screening and hit optimization. *J Med Chem.* 2017;60:6289–6304.
28. Chan-Penebre E, Kuplast KG, Majer CR, et al. A selective inhibitor of PRMT5 with in vivo and in vitro potency in MCL models. *Nat Chem Biol.* 2015;11:432–437.
29. Ye Y, Zhang BD, Mao RF, et al. Discovery and optimization of selective inhibitors of protein arginine methyltransferase 5 by docking-based virtual screening. *Org Biomol Chem.* 2017;15:3648–3661.
30. Ji S, Ma S, Wang WJ, et al. Discovery of selective protein arginine methyltransferase 5 inhibitors and biological evaluations. *Chem Biol Drug Des.* 2017;89:585–598.
31. Duncan KW, Rioux N, Boriack-Sjodin PA, et al. Structure and property guided design in the identification of PRMT5 tool compound EPZ015666. *ACS Med Chem Lett.* 2016;7:162–166.
32. Mavrakis KJ, McDonald 3rd ER, Schlabach MR, et al. Disordered methionine metabolism in MTAP/CDKN2A-deleted cancers leads to dependence on PRMT5. *Science.* 2016;351:1208–1213.
33. Antonysamy S, Bonday Z, Campbell RM, et al. Crystal structure of the human PRMT5:MEP50 complex. *Proc Natl Acad Sci U S A.* 2012;109:17960–17965.
34. Jeong KW, Lee JH, Park SM, et al. Synthesis and in-vitro evaluation of 2-amino-4-arylthiazole as inhibitor of 3D polymerase against foot-and-mouth disease (FMD). *Eur J Med Chem.* 2015;102:387–397.
35. Mo H, He JL, Yuan ZC, et al. WT1 is involved in the Akt-JNK pathway dependent autophagy through directly regulating Gas1 expression in human osteosarcoma cells. *Biochem Biophys Res Commun.* 2016;478:74–80.
36. Gurung B, Hua X. Menin/PRMT5/hedgehog signaling: a potential target for the treatment of multiple endocrine neoplasia type 1 tumors. *Epigenomics.* 2013;5:469–471.